Russian Journal of Earth Sciences

Co- and Pre-Seismic Crustal Deformations Related to Large Earthquakes Between Years of 2009 and 2023 Using Continuous CORS-TR GNSS Observations in the Anatolian Diagonal (Turkey)

P. Dokukin[1], M. A. Güvenaltin[2], V. Kaftan[*,3], M. Toker[4],

[1] People's Friendship University of Russia, Moscow, Russia
[2] Hacettepe University, Ankara, Turkey
[3] Geophysical Center RAS, Moscow, Russia
[4] Yuzuncu Yil University, Van, Turkey
* **Correspondence to:** Vladimir Kaftan, v.kaftan@gcras.ru.

Abstract: Synoptic animations of internal displacements and deformations of the earth's crust were obtained based on the results of continuous GNSS observations in Eastern Anatolia from 2009 to 2023. The spatiotemporal patterns of the seismic deformation process in connection with the tectonics of the region have been identified. It is shown that dilatation and total shear strains evolve in concert with the migration of the strongest earthquakes Elazig, Elazig-Malatya and devastate Karamanmaraş series. Two years before the occurrence of the devastating earthquakes of 2023, a deficit of internal displacements of GNSS stations developed in the area of their epicenters. The conducted research suggests that the strongest events of 2009–2023 are connected by a unitary seismic deformation process. The most important action in this case is the SW movement of the Anatolian block as monolithic element. In the development of movements and deformations, a flow of increasing stresses is observed in the direction from Karliova Triple Junction to the SW to the area of the strongest seismic events on February 2023. It originates east of the Karliova Triple Junction where the Arabian Plate encounters an obstacle. The role of mantle flows in the seismic process is assessed.

Keywords: GNSS, crustal deformation, displacement deficit, earthquake migration, seismo-deformation process, synoptic analysis.

Citation: Dokukin, P., M. A. Güvenaltin, V. Kaftan, and M. Toker (2023), Co- and Pre-Seismic Crustal Deformations Related to Large Earthquakes Between Years of 2009 and 2023 Using Continuous CORS-TR GNSS Observations in the Anatolian Diagonal (Turkey), *Russian Journal of Earth Sciences*, 23, ES5005, EDN: CJREIU, https://doi.org/10.2205/2023es000877

Research Article

Received: 21 September 2023
Accepted: 10 November 2023
Published: 29 December 2023

1. Introduction

The territory of Eastern Anatolia (Turkey) is an area of intense movements and deformations of the earth's crust caused by active tectonic processes and seismic activity. The tectonics of this territory is represented by fault zones with a left-sided shear mechanism. This area is called the Anatolian neotectonic diagonal due to the spatial orientation of the main tectonic faults, extending in the SW–NE direction [*Seyitoğlu et al.*, 2022].

In recent years and decades, a network of continuous GNSS observations has been deployed in Turkey. This circumstance provided the opportunity for an experimental study of recent movements and deformations of the earth's crust in the specified territory for the interval 2009–2023. During this time, several destructive earthquakes occurred in the region. The purpose of this work was to study the spatiotemporal tendencies in the deformation of the earth's crust in connection with strong seismic events in accordance with the tectonic regime of the region.

The study consisted of two stages. The first and main stage was to study the evolution of movements and deformations of the region over the time interval from 2009–2021. About

a year after its completion, in February 2023, a series of destructive doublet earthquake sequences occurred in the SW-section of our study area; the 6th February 2023 ($M7.9$, $M7.6$) earthquake ruptures struck the region, triggering a second event and a cascade of strong aftershocks (~10,000 events) in the Maras Triple Junction (MTJ) [*Toker et al.*, 2023] region of SE-Anatolia. The circumstance associated with the 2023 catastrophic doublets, which redistributed and/or shifted the crustal stresses in the study area, led to further analysis in order to assess co- and pre-seismic displacements and related crustal deformations.

2. Tectonics and Seismicity of the Studied Region

The study region represents the area of interaction between the Nubian and Arabian tectonic plates with the Anatolian block and the Eurasian plate, respectively.

The tectonics of the studied region is represented by the following main tectonic elements (Figure 1). The main tectonic structure is the North Anatolian Fault Zone (NAFZ). This is the main fault zone marking the boundary of the main tectonic plates: the Eurasian and Arabian. This zone, along with the Varto Fault Zone (VFZ), creates an obstacle to the movement of the Arabian Plate to the North, reversing the movement of the lithosphere towards the west-southwest within the segment bounded by the NAFZ and East Anatolian Fault Zone (EAFZ).

The Karliova Triple Junction (KTJ) area is a key feature that determines the nature of tectonic movements in the study region. It is dissected by multiple local faults and includes the volcanic areas of Turnadag and Varto. The feeding of these volcanic centers, as the authors believe, is due to the outcrop of the Anatolian tectonic block to the west-southwest [*Karaoğlu et al.*, 2018]. There is a hypothesis about the existence of a mantle plume east of the KTJ [*Gök et al.*, 2007], the dynamics of which can form an asthenospheric flow that contributes to the removal of the Anatolian block to the west-southwest. The southern end of the East Anatolian Fault Zone from the east limits the area of hypothetical rise of warmer upper mantle, thereby leading to extensional deformation of the earth's crust in the southern part of the Anatolian block [*Gök et al.*, 2007].

Recent GNSS studies show that plate-pulling forces are also characteristic of Western Turkey [*Bartol and Govers*, 2014; *Kutoglu et al.*, 2016; *McClusky et al.*, 2000; *Reilinger et al.*, 2006; *Wei et al.*, 2019]. These studies also suggest that these forces play an important role in the westward movement of the Anatolian Plate.

The main tectonic element in the context of this study is the EAFZ. The EAFZ, one of the most active faults in Turkey, has a NE-SW direction and has a length of approximately 550 km [*Reilinger et al.*, 2006]. The first study on the slip rate of the fault was made by *Taymaz et al.* [1991]. *Taymaz et al.* [1991] determined the slip rate as 29 mm/year for the EAFZ zone. However, current GNSS studies show that the slip rate is around 8–11 mm/year [*Angus et al.*, 2006; *McClusky et al.*, 2000; *Reilinger et al.*, 2006] and our study. *Çetin et al.* [2003] used paleoseismological and historical earthquake records and suggest that there is strain accumulation on the EAFZ. Although the tectonic stress on the EAFZ is mostly accommodated by strike-slip faulting, moreover it is seen that small-medium earthquakes have different focal mechanisms.

The structure of the lithosphere of the studied region is represented by three different structures: the East Anatolian High plateau (further east of the KTJ), the Anatolian block and the northern part of the Arabian plate. The boundaries of the structures are consistent with the main tectonic boundaries. The authors of [*Gök et al.*, 2007] show that the area east of the KTJ is supported by doming hot asthenospheric material resulted from slab delamination and break off process (e.g., beneath Lake Van region in [*Toker and Şahin*, 2019, 2022]).

3. Data and Method

The study used three types of experimental data: faulting, earthquakes, and continuous GPS observations.

Digital data on the position of active faults in the study area were obtained from the source [*Emre et al.*, 2012].

The earthquake catalogue used in this study is retrieved from the Bogaziçi University, Kandilli Observatory and Earthquake Research Institute (KOERI) database [*KOERI, Boğaziçi University*, 2021] and contains instrumental period data (1900–2021). In the subsequent period 2022–2023, we limited ourselves to data on the strongest events, due to too many moderate and weak aftershocks, information about which is not so important for our specific study.

The most important earthquakes of the period under study are presented in the Table 1.

The most important component of experimental data is GNSS observation data. For this study, continuous measurements were used at stations of the Turkish continuously operating network. TUSAGA-Aktif (Continuously Operating Reference Stations-Turkey (CORS-TR) has been continuously measuring with its more than 150 stations since 2009 and obtaining daily observation files within Turkey's borders. Especially recent earthquakes have been monitored by near-area stations [*Irmak et al.*, 2021; *Konca et al.*, 2021; *Yalvac*, 2020].

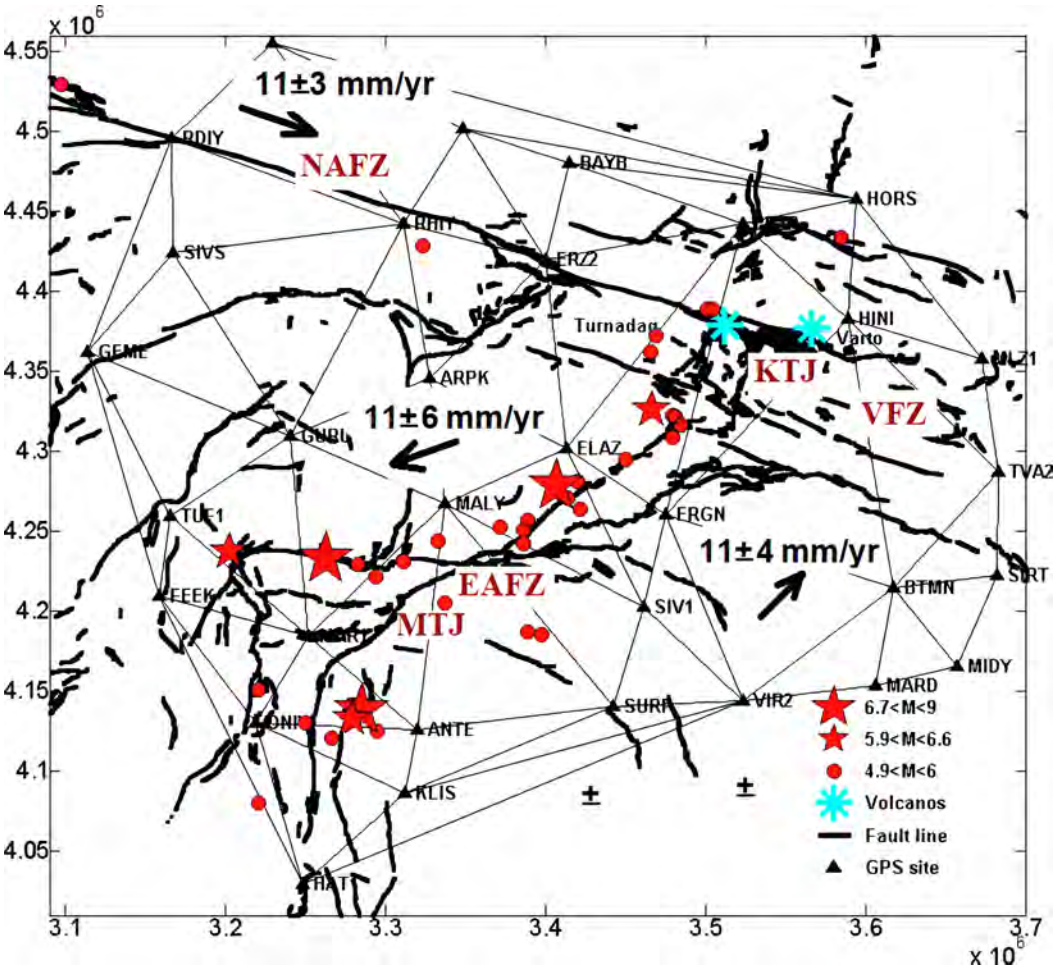

Figure 1. Fault tectonics, major earthquakes, and Delaunay triangulation from GNSS stations participating in the study. Black arrows are the directions of movement of the main tectonic blocks in the internal coordinate reference system. Average movement velocities are calculated for the period 2009–2023. EAFZ – East Anatolian Fault Zone. KTJ – Karliova Triple Junction. NAFZ – North Anatolian Fault Zone. MTJ – Maras Triple Junction. VFZ – Varto Fault Zone. The borders of the frames of the figures here and below indicate rectangular coordinates in the UTM projection, expressed in meters.

Table 1. The most important earthquakes of the period of between years of 2009 and 2023

City	Date, (yyyy.mm.dd)	Time, (h:m:s)	Coordinates, (°C)		Depth, (km)	M_w
			Lat.	Long.		
Elazığ	2010.03.08	02:32:34.710	38.864	39.986	12	6.1
Elazığ, Malatya	2020.01.24	17:55:14.147	38.43120	39.06090	10	6.7
Bingöl	2020.06.14	14:24:29.501	39.42290	40.70730	10	5.9
Bingöl	2020.06.15	06:51:31.776	39.42260	40.74790	10	5.5
Gaziantep	2023.02.06	01:17:35	37.112	37.119	17.9	7.8
Nuradagi	2023.02.06	01:28:15	37.127	36.943	12.2	6.7
Kahramanmaraş	2023.02.06	10:24:49	38.024	37.203	10.0	7.5
Dogansehir	2023.02.06	10:35:38	38.008	37.751	8.1	6.0

In the first part of the study, 32 of these stations' time series have been examined. In order for the observation files to be interpreted geometrically, they must go through post-processing. From the beginning of 2022, the Turkish General Mapping Directorate started to share the daily results and time series obtained from observation files of these stations (https://www.harita.gov.tr/public/sunum/). The aforementioned post-processing was provided by this institution and it is known that the open-source GAMIT/GLOBK software is used [*Herring et al.*, 2018]. The final solution is computed in ITRF2014 datum. While processing daily observation files, IGS (International GNSS Service) stations have been used for regional stabilization [*Kurt et al.*, 2020].

The network used in the study is shown in Figure 1. An important circumstance is that before and after the catastrophic earthquakes in Eastern Anatolia, some GNSS stations were moved from their original locations. The following stations have been moved and renamed as BAYB-BYB1, GEME-GEM1, HAT1-HAT2, KLIS-KLS1, MALY-MLY1, SIRT-SRT1, SIVS-SVS1. To obtain a continuous history of movements and deformations of the earth's crust, the time series of the previous stations were extended by observations at their new analogues, taking into account the local mutual increments of coordinates obtained as soon as possible after the completion of the operation of these relocated stations. We allowed such laxity on the basis that all new analogues of GNSS stations are installed in the territories of the same consolidated blocks at a considerable distance from moving faults. Most stations are mutually distant by no more than km. BAYB and MALY stations have been moved by 5.5 and 8.6 km, respectively. However, they did not cease to be on the same consolidated block.

On dates of technical breaks in observations, in order to avoid irregularity of time series, the missing coordinates were determined by interpolation with Hermite splines.

4. Analysis of Internal Movements and Deformations of the Earth's Crust

Horizontal displacements of GNSS sites are calculated for the every daily coordinate solution. Time series of horizontal displacements U_n and U_e in a reference to the initial epoch T_0 as horizontal coordinate differences n and e in UTM projection were received by the formulas

$$U_{n_i} = n_i - n_0,\ U_{e_i} = e_i - e_0,$$

where index i denotes the current epoch (day) of measurements.

Displacements of GNSS points, expressed in a global reference system, demonstrate first of all the trends in the movement of the global tectonic plate on which the observation point is located. This effect makes it difficult to track movements associated with local changes, such as the slow accumulation of elastic deformations in the Earth's crust near the epicenter of a future event. In this case, more indicative characteristics of the movements

are the displacements of points, presented in the local (internal) reference system, which well reflect the mutual multidirectional movements of the sides of local faults. The rationale for this approach is presented in [*Gvishiani et al.*, 2022]. Such a local (internal) displacement reference system can be easily obtained by subtracting from each displacement U_j in the global reference system the average value $\overline{U}$, which characterizes the trend of global tectonics common to all network points, for each epoch measurements. Thus, we obtain a reference system for displacements (or displacement rates) according to the well-known no net translation principle

$$u_{n_j} = U_{n_j} - \overline{U_n},\ u_{e_j} = U_{e_j} - \overline{U_e},$$

where index j is the current number of the GNSS observation point.

For each day of observation, based on the displacement values, we obtained digital models of the distribution of horizontal deformations of total shear and dilatation. These characteristics are invariant with respect to the choice of coordinate system. The spatial models were motion and deformation characteristics interpolated onto a regular 1 km grid using Hermite splines.

To calculate the deformations of the finite elements, the horizontal deformation tensor was used (the n and e axes are directed to the north and east)

$$T_\varepsilon = \begin{pmatrix} \varepsilon_n & \varepsilon_{ne} \\ \varepsilon_{en} & \varepsilon_e \end{pmatrix},$$

whose elements were equal $\varepsilon_n = \frac{\partial u_n}{\partial n}$, $\varepsilon_e = \frac{\partial u_e}{\partial e}$ and $\varepsilon_{en} = \varepsilon_{ne} = \frac{1}{2}\left(\frac{\partial u_n}{\partial e} + \frac{\partial u_e}{\partial n}\right)$, correspondently, where $\left(\frac{\partial u_n}{\partial e} + \frac{\partial u_e}{\partial n}\right) = \gamma_{ne} = \gamma_{en}$ – relative shear.

Elements of the strain tensor are represented by the partial derivatives of the displacements u_n and u_e along the coordinate axes n and e.

To study the spatiotemporal distribution of horizontal deformations, the following invariant characteristics were calculated.

1) Principal strains ε_1 and ε_2 $\varepsilon_{1,2} = \frac{1}{2}\left[\varepsilon_n + \varepsilon_e \pm \sqrt{(\varepsilon_n - \varepsilon_e)^2 + \gamma_{ne}^2}\right]$.
2) Total shear $\gamma = \left((\varepsilon_n - \varepsilon_e)^2 + \gamma_{ne}^2\right)^{1/2}$.
3) Dilatation $\Delta = \varepsilon_1 + \varepsilon_2$.

The strain components were calculated using the method described in [*Wu et al.*, 2006].

Due to the significant non-equivalence of the finite elements (see Figure 1), the deformation values were reduced to the average square of the network triangle [*Kaftan and Melnikov*, 2019].

Spatial models of movements and deformations obtained for each day were combined into evolutionary models – video animations of the seismic deformation process. All video images show active fault lines. The epicenters of earthquakes were plotted on the frames starting from the date of their occurrence. Thus, a basis was obtained for a heuristic analysis of the spatiotemporal relationship between fault tectonics, seismicity, movements and deformations of the study area.

5. Study of the Evolution of Seismotectonic Movements and Crustal Deformations

5.1. Horizontal Dilatation Strain

Analysis of the characteristics of areal extension and compression is aimed primarily at assessing the behavior of subcrustal currents and the temperature regime of the asthenosphere. But at the same time, significant dilatation anomalies are formed due to the release of accumulated seismic energy at the source of a strong earthquake. Long-term and continuous GNSS observations make it possible to test modern concepts in the field of tectonics and geodynamics. The evolution of dilatation strain from 2009 to 2023 can

be observed in video animation [*Kaftan et al.*, 2023a]. Selected key frames covering the catastrophic earthquakes of 2023 are presented in Figure 2.

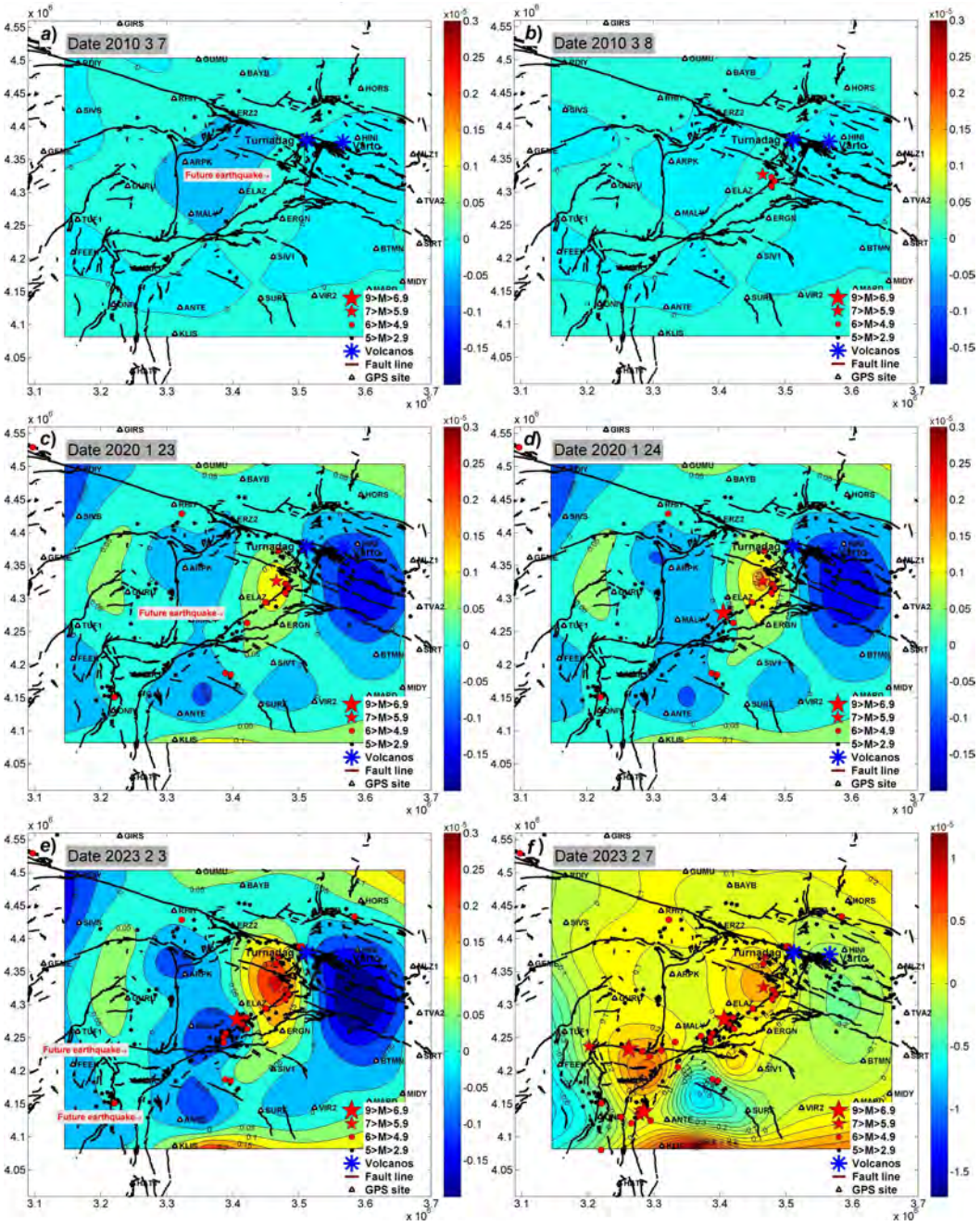

Figure 2. Evolution of dilatation deformation 2009–2023 in connection with the strongest seismic events.

Visual analysis shows that the first strong seismic event $M6.1$ in 2010 was not significantly manifested by changes in dilatational deformation. Approximately two years after this event, significant compressive strains began to develop in the VFZ region. Following this event, in the area of the epicenter, about a year later, an extreme areal extension formed, which began to develop without being accompanied by noticeable seismic activity. The area of horizontal extension expanded until the main seismic event $M6.7$ in 2020. This earthquake occurred at the boundary of the interaction of compression and extension areas, revealing the shear mechanism of seismic rupture. A destructive series of moderate Bingol earthquakes in the second half of 2020 also occurred at the boundary of the interaction

of the main extrema of extension and compression in the north of the KTJ. The main extremum of extension in the southwestern part of the KTJ fault series appears to be the main source of tectonic deformation that determines the spatiotemporal distribution of the stress pattern. The extremum of tensile stresses contributes to the movement of the Anatolian block in the earth's crust to the southwest. After the catastrophic earthquakes of Eastern Anatolia 2023, the entire territory of the Eastern Anatolian block between the main seismic ruptures experienced significant horizontal extension.

5.2. Total Shear Deformation Analysis

In regions with a predominant shear mechanism of movements along active faults, slow deformation shear waves are detected [*Kaftan and Melnikov*, 2019; *Kaftan and Tatarinov*, 2022]. This prompted the idea to investigate this phenomenon in the Eastern Anatolia region. Based on the results of processing GNSS observations, video animations of the full shear deformation were obtained [*Kaftan et al.*, 2023b]. Key frames are shown in Figure 3.

Visual synoptic analysis allows us to discover new patterns of seismicity and cause-and-effect relationships in the evolution of the seismic-deformation process. It can be seen that approximately a year before the strong earthquake $M6.1$ (August 3, 2010), a significant deformation extremum of 2.5×10^{-6} was formed in the area of the future epicenter (Figure 3a). This indicates that a strong earthquake is caused by the accumulation of shear deformations that contribute to the release of stress within a mature seismic source. The subsequent development of the deformation process shows an increase and spread of deformation to the southwest along the EAFZ, as well as to the northwest along the NAFZ. At the same time, moderate seismic events with $M \sim 5$ occur in the area of deformation propagation. The main part of them migrates, following the deformation flow, to the epicenter of the future strong earthquake Elazig-Malatya on January 24, 2020 $M6.7$. This creates a trimodal region of extremes of the total shear strain. An earthquake occurs in a trough between two local maxima of deformation. The main shock promotes the merging of two local deformation extrema into a single region extended along the EAFZ. An interesting feature is the formation of a local maximum of deformation on the northwestern border of the study area, in which two moderate seismic events occurred. Visual analysis allows one to observe the seismic deformation process and draw conclusions about the mechanisms of stress accumulation and release during strong earthquakes, as well as the role of the Karliova Triple Junction as an intersection point of the study area. From this area, the propagation of total shear deformation continued directly towards the epicenter of the first devastate earthquake of Eastern Anatolia 2023 (Figure 3e). This circumstance suggests that the second strongest earthquake of the February 2023 series was a consequence of the first.

5.3. Deficit of Internal Movements Due to Strong Earthquakes

Having long-term data on the nature of crustal movements in the study area, we analyzed the accumulation trends of the module of vectors of internal movements of GPS points. The corresponding synoptic animation is presented in [*Dokukin et al.*, 2023; *Kaftan et al.*, 2023c]. Key frames of the animation are shown in Figure 4.

The experience of similar studies has shown that a minimum of internal displacements accumulates before strong earthquakes in the area of their epicenter [*Kaftan*, 2021; *Kaftan et al.*, 2022]. We consider this characteristic as a predictor of the location of a future earthquake as a place that impedes general movement.

The presented synoptic video demonstrates the evolution of the deficit of internal displacements in the area of occurrence of a set of strong earthquakes in Elazig (Turkey) in 2009–2021. It can be seen that the first strong seismic event of 2010 with $M6.1$ occurred in a zone of deficiency of internal displacements, expressed in dark brown. Subsequently, an increase in internal displacements occurred in this place, accompanying the release and relaxation of elastic stresses. The area of internal displacement deficit has shifted in two directions to the southwest and northwest along the distribution of the NAFZ and EAFZ.

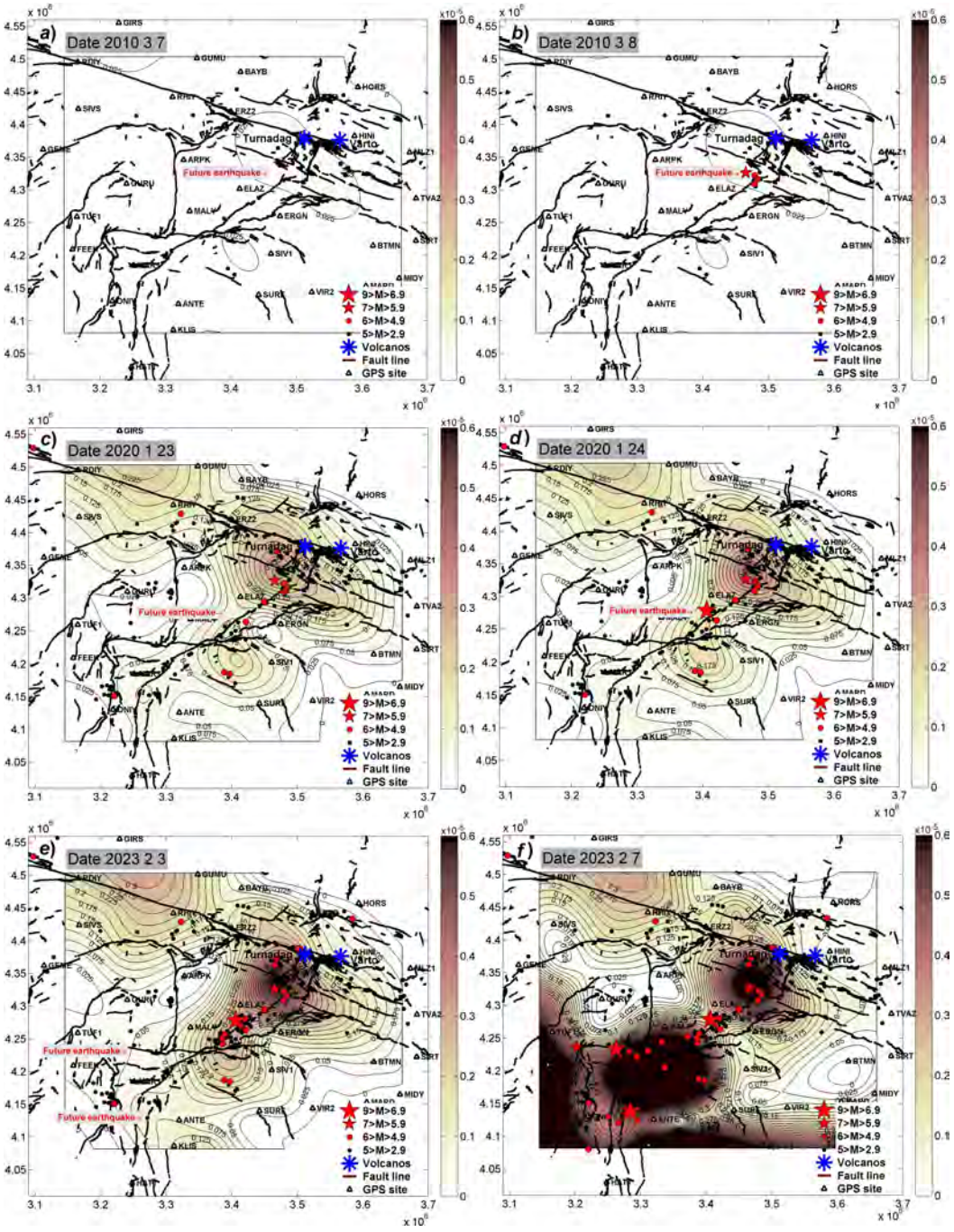

Figure 3. Evolution of the total shear deformation 2009–2023 in connection with the strongest seismic events.

Subsequently, four moderate earthquakes with $M \sim 5$ occurred in these areas. Two of them, located to the southeast of the EAFZ, caused increased mobility of the earth's crust at the epicenter of the strongest earthquake of 2020 with $M6.7$. The 2020 Elazig earthquake occurred in a zone of accumulated displacements at a level of 5–6 cm and was accompanied by a co-seismic displacement of more than 10 cm, which subsequently increased to 13 cm. A series of destructive Bingol earthquakes in 2020 also occurred in the mobile zone. In the subsequent period, the entire study area was subjected to accumulated displacements of at least 5 cm. This indicates a release of elastic pre-seismic stresses throughout this area.

Starting from 2020, a minimum of local internal displacements has formed in the southwestern territory of the region. It existed until the occurrence of a series of strong

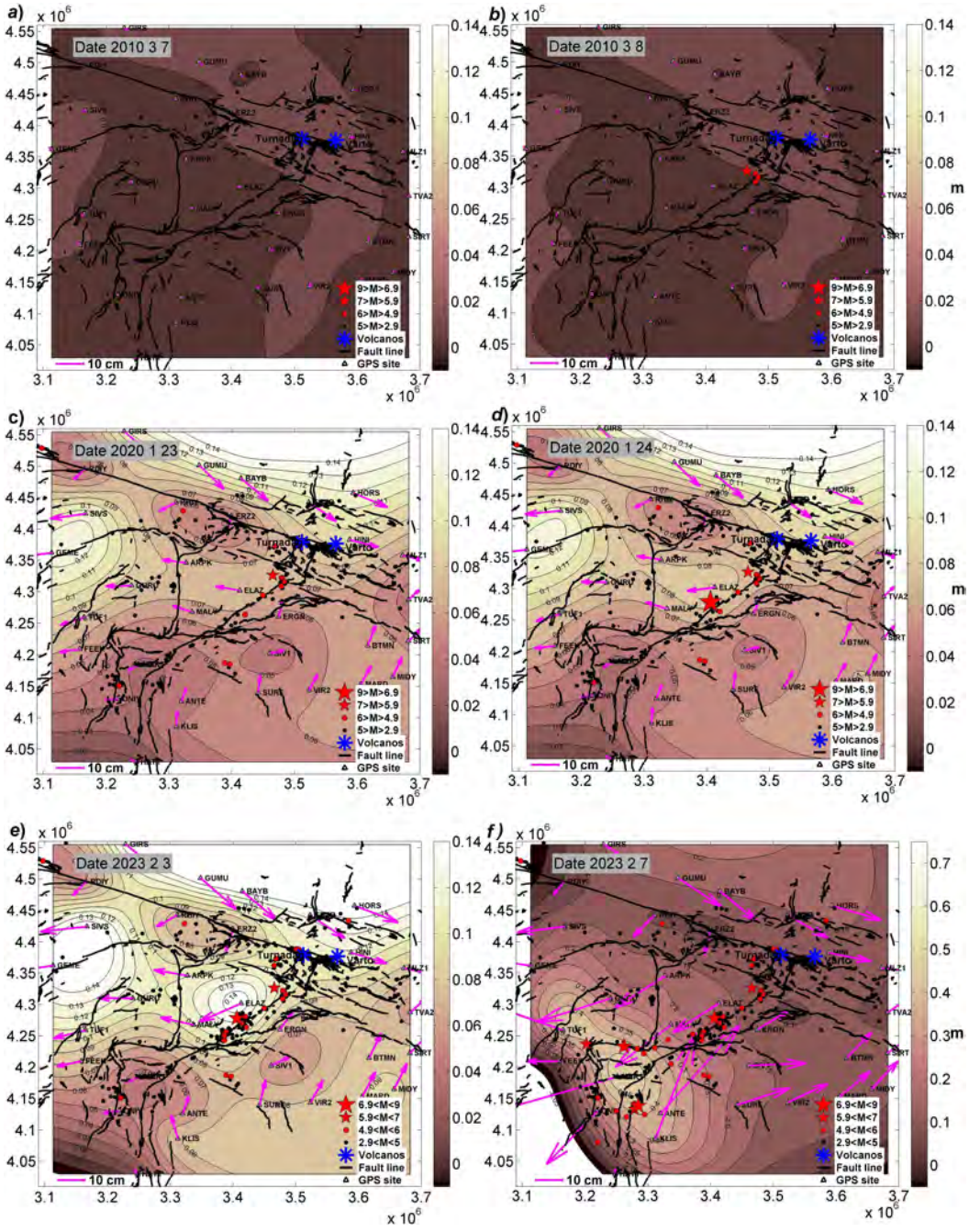

Figure 4. Evolution of the internal displacement deficit 2009–2023.

earthquakes in 2023, which occurred within this minimum. This result once again showed that the analysis of the deficit of internal displacements is very promising in solving the problem of predicting the location of strong earthquakes.

6. Discussion and Conclusion

In the present study, we attempt to show the spatial and temporal nature of periods of complete deformation through a synopsis of ongoing tectonism in the study area, to understand how horizontal vectors and deformation are consistent with the relative movements of the Anatolian and Arabian blocks. Spatial and temporal patterns of geodetic deformation evolution highlight a new perspective on KTJ. A new view is being formed on the KTJ as a source of stress propagation that determines the kinematics of the East Anatolian block. The concentration of subcrustal stresses occurs due to the collision of

the Arabian plate with the Eurasian plate in the VFZ. In this area, maximum compressive deformation is observed, which contributes to the formation of subcrustal lithospheric flows from the KTJ within the framework defined by the NAFZ and EAFZ. These currents in turn create an area of expansion at the southwestern end of the KTJ. Interestingly, this propagation of dilatation strain, framed by KTJ and Anatolian block deformation, obliquely points the Anatolian block to the SW rather than to the NW (or to the W), with strong support for strike-slip and fault deformation. Our main results are in good agreement with the orientations of maximum principal horizontal stresses published in the World Stress Map (WSM2016) and 3D deformation models published in previous studies [e.g., *Kutoglu et al.*, 2016]; the direction of maximum principal stress, oriented generally to the southwest, forms normal and strike-slip faults that extend prominently toward the southwestern end of the Anatolian block into the Maras Triple Junction (MTJ). Comparison of the calculated geodetic and seismic strains from WSM2016 with previously published results shows that the estimated tensile, compressive, and shear strain trajectories are kinematically correlated with MTJ and KTJ. This completes the southwest-directed oblique "transtensional" extrusion of the bilaterally locked Anatolian block, parallel/subparallel to the EAFZ and the Dead Sea Fault (DSF). This may be the reason why the left-lateral earthquake ruptures on February 6, 2023 (M_w 7.7, 7.6) occurred in the area of MTJ.

Synoptic analysis of the evolution of total shear deformation allowed us to trace the flow of shear deformation from the KTJ, through the epicenters of large earthquakes to the southwest, up to the sites of the occurrence of a series of destructive earthquakes in Eastern Anatolia in February 2023. The maximum total shear strain occurred before the 2010 (Figure 3a,b) Elazig earthquake in the vicinity of its epicenter. From this area, shear deformation began to grow naturally along the NAFZ and EAFZ strike routes. It intensified in the area where the 2020 Elazig-Malatya earthquake occurred and continued southeast to the places of the 2023 East Anatolian earthquakes. An analysis of the evolution of the internal displacement deficit has shown the effectiveness of this characteristic for identifying the locations of strong earthquakes. A deficit of internal displacements is formed when it encounters an obstacle to movement in the area of increasing stress.

The conducted research suggests that the strongest events of 2009–2023 are connected by a unitary seismic deformation process. The most important action in this case is the SW movement of the Anatolian block as monolithic element. In the development of movements and deformations, a flow of increasing stresses is observed in the direction from KTJ to the SW to the area of the strongest seismic events on February 2023. It originates east of the KTJ where the Arabian Plate encounters an obstacle. We assume here the presence of a branch to the SW from the sublithospheric flow, pulling the Arabian plate mainly to the north.

Finally, our results conclude that the knowledge of the co- and pre-seismic crustal deformation patterns compared with the large recent earthquakes (2009 to 2023) in the Anatolia provides very important information on the location of the main faults, earthquakes and strain accumulation for seismic hazard assessment [e.g., *Kutoglu et al.*, 2016]. This motivates an agreement between the seismic and tectonic strains, which confirm that there are seismically active crustal deformations in Anatolia.

Acknowledgments. The work was carried out within the framework of the state assignment of the Geophysical Center of the Russian Academy of Sciences, approved by the Ministry of Science and Higher Education of the Russian Federation, and also within the working plans of Hacettepe University (Ankara) and Yuzuncu Yil University (Van) Geophysics Division, Turkey.

The authors would like to express their gratitude to the General Directorate of Mapping (from the Republic of Türkiye's Ministry of National Defence) for providing valuable daily GNSS observation data. This data, shared openly through their database, was instrumental in conducting the research presented in this article. The accessibility and quality of the data significantly contributed to the accuracy and reliability of our findings. We thank the distinguished reviewers for their careful reading of the manuscript and helpful recommendations for its improvement.

References

Angus, D. A., D. C. Wilson, E. Sandvol, and J. F. Ni (2006), Lithospheric structure of the Arabian and Eurasian collision zone in eastern Turkey from S-wave receiver functions, *Geophysical Journal International*, *166*(3), 1335–1346, https://doi.org/10.1111/j.1365-246X.2006.03070.x.

Bartol, J., and R. Govers (2014), A single cause for uplift of the Central and Eastern Anatolian plateau?, *Tectonophysics*, *637*, 116–136, https://doi.org/10.1016/j.tecto.2014.10.002.

Çetin, H., H. Güneyli, and L. Mayer (2003), Paleoseismology of the Palu-Lake Hazar segment of the East Anatolian Fault Zone, Turkey, *Tectonophysics*, *374*(3–4), 163–197, https://doi.org/10.1016/j.tecto.2003.08.003.

Dokukin, P., M. A. Guvenaltin, T. S. Irmak, V. Kaftan, and M. Toker (2023), Evolution of the crustal inner displacement deficit in a reference to Elazig earthquake series just before occurring the devastate Ekinozu-Nuradagi earthquakes (M7.5–7.8, 2023-02-06), https://doi.org/10.2205/ESDB-Ekinozu-Nurdagi-quakes.

Emre, O., T. Y. Duman, and H. Elmacı (2012), 1:250 000 Scale Active Fault Map Series of Turkey.

Gök, R., M. E. Pasyanos, and E. Zor (2007), Lithospheric structure of the continent-continent collision zone: eastern Turkey, *Geophysical Journal International*, *169*(3), 1079–1088, https://doi.org/10.1111/j.1365-246X.2006.03288.x.

Gvishiani, A. D., V. N. Tatarinov, V. I. Kaftan, A. I. Manevich, V. A. Minaev, S. A. Ustinov, and R. V. Shevchuk (2022), Geodynamic Model of the Northern Part of the Nizhnekansk Massif: Fault Tectonics, Deformations, and Insulation Properties of Rock Displacements, *Doklady Earth Sciences*, *507*(1), 909–915, https://doi.org/10.1134/S1028334X22600608.

Herring, T. A., M. A. Floyd, R. W. King, and S. C. McClusky (2018), *Global Kalman filter VLBI and GPS Analysis Program, GLOBK Reference Manual, Release 10.6. Department of Earth, Atmospheric and Planetary Sciences*, Massachusetts Institute of Technology, Cambridge, MA.

Irmak, T. S., M. Toker, E. Yavuz, E. Şentürk, and M. A. Güvenaltın (2021), New insight into the 24 January 2020, Mw 6.8 Elazığ earthquake (Turkey): An evidence for rupture-parallel pull-apart basin activation along the East Anatolian Fault Zone constrained by Geodetic and Seismological data, *Annals of Geophysics*, *64*(4), https://doi.org/10.4401/ag-8638.

Kaftan, V., and A. Melnikov (2019), *Migration of Earth Surface Deformation as a Large Earthquake Trigger*, pp. 71–78, Springer International Publishing, https://doi.org/10.1007/978-3-030-31970-0_8.

Kaftan, V., P. Dokukin, M. A. Guvenaltin, M. Toker, and T. S. Irmak (2023a), Fifteen-year evolution of the crustal dilatation in a reference to the recent East Anatolian earthquakes, https://doi.org/10.2205/ESDB-000877-d01.

Kaftan, V., P. Dokukin, M. A. Guvenaltin, M. Toker, and T. S. Irmak (2023b), Fifteen-year evolution of the crustal total shear strain in a reference to the recent East Anatolian earthquakes, https://doi.org/10.2205/ESDB-000877-d02.

Kaftan, V., P. Dokukin, M. A. Guvenaltin, M. Toker, and T. S. Irmak (2023c), Fifteen-year evolution of the crustal inner shear deficit in a reference to the recent East Anatolian earthquakes, https://doi.org/10.2205/ESDB-000877-d03.

Kaftan, V. I. (2021), An Analysis of Ground Movements and Deformations from 13-Year GPS Observations before and during the July 2019 Ridgecrest, USA Earthquakes, *Journal of Volcanology and Seismology*, *15*(2), 97–106, https://doi.org/10.1134/S0742046321010115.

Kaftan, V. I., and V. N. Tatarinov (2022), Registration of Slow Deformation Waves According to GNSS Observations, *Doklady Earth Sciences*, *505*(1), 489–495, https://doi.org/10.1134/S1028334X22070091.

Kaftan, V. I., V. N. Tatarinov, and R. V. Shevchuk (2022), Long-term changes in crustal movements and deformations before and during the 2016 Kumamoto earthquake sequence, *Geodynamics & Tectonophysics*, *13*(1), https://doi.org/10.5800/GT-2022-13-1-0570.

Karaoğlu, O., J. Browning, M. K. Salah, A. Elshaafi, and A. Gudmundsson (2018), Depths of magma chambers at three volcanic provinces in the Karlıova region of Eastern Turkey, *Bulletin of Volcanology*, *80*(9), https://doi.org/10.1007/s00445-018-1245-x.

KOERI, Boğaziçi University (2021), Kandilli Observatory and Earthquake Research Institute, Regional Earthquake-Tsunami Monitoring Center: Earthquake Catalogue, http://www.koeri.boun.edu.tr/sismo/zeqdb/, (date of access: 01/12/2021).

Konca, A. O., H. Karabulut, S. E. Güvercin, F. Eskiköy, S. Özarpacı, A. Özdemir, M. Floyd, S. Ergintav, and U. Doğan (2021), From Interseismic Deformation With Near-Repeating Earthquakes to Co-Seismic Rupture: A Unified View of the 2020 Mw6.8 Sivrice (Elazığ) Eastern Turkey Earthquake, *Journal of Geophysical Research: Solid Earth*, *126*(10), https://doi.org/10.1029/2021JB021830.

Kurt, A. İ., A. Cingöz, S. Özdemir, S. Peker, Ö. Özel, and M. Simav (2020), Türkiye Ulusal Temel GNSS Ağı (TUTGA) Güncel Koordinat ve Hızlarının GNSS Verilerinin Yeniden Değerlendirilmesi Kapsamında Hesaplanması, *Harita Dergisi*, *164*, 1–17.

Kutoglu, H. S., M. Toker, and C. Mekik (2016), The 3-D strain patterns in Turkey using geodetic velocity fields from the RTK-CORS (TR) network, *Journal of African Earth Sciences*, *115*, 246–270, https://doi.org/10.1016/j.jafrearsci.2015.12.002.

McClusky, S., S. Balassanian, A. Barka, C. Demir, S. Ergintav, I. Georgiev, O. Gurkan, M. Hamburger, K. Hurst, H. Kahle, K. Kastens, G. Kekelidze, R. King, V. Kotzev, O. Lenk, S. Mahmoud, A. Mishin, M. Nadariya, A. Ouzounis, D. Paradissis, Y. Peter, M. Prilepin, R. Reilinger, I. Sanli, H. Seeger, A. Tealeb, M. N. Toksöz, and G. Veis (2000), Global Positioning System constraints on plate kinematics and dynamics in the eastern Mediterranean and Caucasus, *Journal of Geophysical Research*, *105*(B3), 5695–5719, https://doi.org/10.1029/1996JB900351.

Reilinger, R., S. McClusky, P. Vernant, S. Lawrence, S. Ergintav, R. Cakmak, H. Ozener, F. Kadirov, I. Guliev, R. Stepanyan, M. Nadariya, G. Hahubia, S. Mahmoud, K. Sakr, A. ArRajehi, D. Paradissis, A. Al-Aydrus, M. Prilepin, T. Guseva, E. Evren, A. Dmitrotsa, S. V. Filikov, F. Gomez, R. Al-Ghazzi, and G. Karam (2006), GPS constraints on continental deformation in the Africa-Arabia-Eurasia continental collision zone and implications for the dynamics of plate interactions, *Journal of Geophysical Research: Solid Earth*, *111*(B5), https://doi.org/10.1029/2005JB004051.

Seyitoğlu, G., E. Tunçel, B. Kaypak, K. Esat, and E. Gökkaya (2022), The Anatolian Diagonal: a broad left lateral shear zone between the North Anatolian Fault Zone and the Aegean / Cyprus Arcs, *Türkiye Jeoloji Bülteni / Geological Bulletin of Turkey*, *65*(2), 93–116, https://doi.org/10.25288/tjb.1015537.

Taymaz, T., H. Eyidoğan, and J. Jackson (1991), Source parameters of large earthquakes in the East Anatolian Fault Zone (Turkey), *Geophysical Journal International*, *106*(3), 537–550, https://doi.org/10.1111/j.1365-246X.1991.tb06328.x.

Toker, M., and Ş. Şahin (2019), Crustal Poisson's ratio tomography and velocity modeling across tectono-magmatic lake regions of Eastern Anatolia (Turkey): New geophysical constraints for crustal tectonics, *Journal of Geodynamics*, *131*, 101,651, https://doi.org/10.1016/j.jog.2019.101651.

Toker, M., and Ş. Şahin (2022), Upper- to mid-crustal seismic attenuation structure above the mantle wedge in East Anatolia, Turkey: Imaging crustal scale segmentation and differentiation, *Physics of the Earth and Planetary Interiors*, *329–330*, 106,908, https://doi.org/10.1016/j.pepi.2022.106908.

Toker, M., E. Yavuz, M. Utkucu, and F. Uzunca (2023), Multiple segmentation and seismogenic evolution of the 6th February 2023 (*Mw* 7.8 and 7.7) consecutive earthquake ruptures and aftershock deformation in the Maras triple junction region of SE-Anatolia, Turkey, *Physics of the Earth and Planetary Interiors*, *345*, 107,114, https://doi.org/10.1016/j.pepi.2023.107114.

Wei, W., D. Zhao, F. Wei, X. Bai, and J. Xu (2019), Mantle Dynamics of the Eastern Mediterranean and Middle East: Constraints From P-Wave Anisotropic Tomography, *Geochemistry, Geophysics, Geosystems*, *20*(10), 4505–4530, https://doi.org/10.1029/2019GC008512.

Wu, J. C., H. W. Tang, Y. Q. Chen, and Y. X. Li (2006), The current strain distribution in the North China Basin of eastern China by least-squares collocation, *Journal of Geodynamics*, *41*(5), 462–470, https://doi.org/10.1016/j.jog.2006.01.003.

Yalvac, S. (2020), Determining the Effects of the 2020 Elazığ-Sivrice/Turkey (Mw 6.7) Earthquake from the Surrounding CORS-TR GNSS Stations by means of Relative GNSS Analysis, *Turkish Journal of Geosciences*, *1*(1), 15–21.